Bulk Acoustic Wave-Mediated Multiferroic Antennas: Architecture and Performance Bound

Zhi Yao, *Student Member, IEEE*, Yuanxun Ethan Wang, *Senior Member, IEEE*, Scott Keller, and Gregory P. Carman

***Abstract*—Time-varying magnetic flux can be induced from the dynamic mechanical strain of acoustic waves in multiferroic devices that are comprised of piezoelectric and magnetostrictive material. Such devices can be used to create electromagnetic radiation and to alleviate the platform effect associated with low-profile conformal antennas. In this paper, a bulk acoustic wave (BAW)-mediated multiferroic antenna structure is proposed. Its potential for efficient radiation of electromagnetic waves is evaluated by analytically deriving the lower bound of its radiation quality factor (Q factor). A one-dimensional (1-D) multiscale finite-difference time-domain (FDTD) technique is developed to predict the bilateral, dynamic coupling between the acoustic waves and electromagnetic waves. The simulation shows a decaying stress profile in the BAW resonator structure, which implies that the radiation of the electromagnetic waves acts as a damping load to the acoustic resonance. The simulated radiation Q factor matches well with the analytical derivations and the agreement validates both the operating principle of the proposed antenna and the FDTD algorithm developed. The study concludes that efficient antennas may be realized at GHz frequencies with thin film multiferroic material that has thicknesses of the order of 10^{-5} wavelength.**

***Index Terms*—Bulk acoustic waves (BAW), conformal antennas, film bulk acoustic resonators (FBARs), finite-difference time-domain (FDTD) method, multiferroic antennas, multiferroic material, platform effect.**

I. Introduction

TRADITIONAL antennas such as dipoles and loops generate propagating electromagnetic waves from conductive currents exposed in free space. Such antennas, however, radiate poorly when placed at a short distance above a conducting plane. This is because an image current flowing in the opposite direction is generated by the platform and it cancels the radiation of the original antenna. The platform effect is also described by the excessive storage of reactive energy between the radiating element and the platform, which elevates the radiation Q factor and makes the antenna difficult to match [1], [2].

Using magneto-dielectric material to reduce the high radiation Q factor associated with the platform effect has been extensively studied in [3]–[9], where optimization of the bandwidth and efficiency performance of specific antenna structures, such as microstrip patch antennas, have been discussed. The use of both natural magnetic material [6]–[8] and artificial magnetic material [9] to alleviate the platform effect has been considered. Recently, the emergence of multiferroic material that couples electric field, magnetic field, and mechanical field has received great attention [10]–[15]. In particular, strain coupled composites of piezoelectric and magnetostrictive phases can link electric field and the magnetic fields to exhibit the giant multiferroic coupling needed for practical applications [14]. It has been proposed to utilize such composite multiferroic materials to miniaturize the RF antenna dimensions because they exhibit high permittivity and high permeability simultaneously [16]. Another application of composite multiferroic material is to create frequency reconfigurable antennas by altering the magnetic properties of the material with electric field [17].

In this paper, a new class of antennas called strain-mediated multiferroic antennas is investigated [18]. Such antennas use the dynamic coupling properties of composite multiferroic materials rather than the static tunability examined in previous works. Dynamic electric flux (displacement current) or magnetic flux is utilized in place of conductive current as the radiation source of the proposed multiferroic antennas. To achieve this, dynamic strain is induced in a thin piezoelectric or piezomagnetic plate to generate a dynamic flux density, which then forms the aperture field on the surface of the plate. This aperture field results in outgoing electromagnetic waves. For example, electromagnetic radiation may be created through vibrating a piezoelectric plate mechanically, as envisioned and formulated in [19]–[22].

Strain-mediated antennas offer several potential advantages compared to conductive-current-based antennas. First, the Ohmic loss associated with the current conduction is absent, which promises superior radiation efficiency. Second, the platform effects may be overcome if strain-mediated magnetic flux is used as the radiation source flowing above the conducting platform. This is because the image effect from the conducting platform enhances rather than cancels the radiation effects of the magnetic flux. Third, strain-mediated antennas can be designed with minimum or no conductive elements over a conducting ground plane, which helps to achieve low observability and high robustness against strong interferences. On the other hand, one must realize that generating and coupling a dynamic strain at RF frequency into a device is not a trivial task. The distribution of strain is often not uniform, as dynamic mechanical vibrations may generate acoustic waves that can propagate, scatter, and radiate in or out of the structure. These effects

Manuscript received August 12, 2014; revised May 02, 2015; accepted May 04, 2015. Date of publication May 11, 2015; date of current version July 31, 2015. This work was supported by the U.S. National Science Foundation under Cooperative Agreement Award EEC-1160504.

Z. Yao and Y. E. Wang are with the Department of Electrical Engineering, University of California, Los Angeles, CA 90024 USA (e-mail: zhiyao@ucla.edu).

S. Keller and G. P. Carman are with the Department of Mechanical and Aerospace Engineering, University of California, Los Angeles, CA 90024 USA.

Color versions of one or more of the figures in this Paper are available online at http://ieeexplore.ieee.org.

Digital Object Identifier 10.1109/TAP.2015.2431723

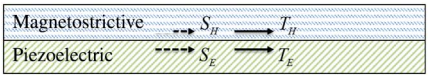

Fig. 1. Composite multiferroic structure formed by lamination of one layer of piezoelectric film and one layer of magnetostrictive layer.

cannot be ignored once the structure dimension is comparable to the acoustic wavelength, which is on the order of several micrometers. Therefore, generation and propagation of acoustic waves must always be considered.

The objectives of this paper are threefold. First, a strain-mediated antenna structure is proposed as a vehicle to study how the platform effects can be overcome by decreasing the radiation Q factor with the multiferroic coupling. The proposed antenna structure consists of a sandwich of two layers of piezoelectric material and one layer of magnetostrictive material, and it relies on bulk acoustic wave (BAW) resonances [23], [24] to transfer the dynamic strain across different layers. Analyses show how the radiation quality factor can be reduced with a high figure of merit for magnetomechanical coupling and a high permeability of the magnetostrictive material. This will lead to low-profile antennas with high radiation efficiency. The second objective is to develop a multiphysics and multiscale modeling tool to emulate the dynamic, two-way interactions between electromagnetic waves and acoustic waves. The model incorporates the fundamental laws of electrodynamics, Maxwell's equations, and elastodynamics, Newton's equations. A one-dimensional (1-D) finite-difference time-domain (1-D FDTD) technique [25]–[29] is developed for this purpose, where Newton's law and Maxwell's equations are solved jointly in time domain. The dynamic response of the stress profile is simulated and the radiation Q factor is derived from it. The radiation Q is then compared to analytical results. The third purpose is to identify the material properties required for practical implementation of multiferroic antennas through modeling.

It is concluded that it is possible to construct a multiferroic antenna, only a few micrometers thick, providing that the magnetic material has relative permeability of several thousand and the magnetomechanical coupling figure of merit is greater than 85%. Furthermore, such an antenna can be placed on top of a conducting plane eliminating the platform effect.

II. Multiferroic Constitutive Relations

A typical configuration for a multiferroic composite is laminated piezoelectric and magnetostrictive layers, as shown in Fig. 1. The bond between the layers is assumed to be perfect, so that the mechanical strain is continuous across the interface. The multiferroic constitutive relationship is then described by the following equations [23]:

$$\begin{bmatrix} \overline{\overline{S}}_E \\ \overline{D} \end{bmatrix} = \begin{bmatrix} s_E & d_E \\ d_E & \varepsilon_T \end{bmatrix} \begin{bmatrix} \overline{\overline{T}}_E \\ \overline{E} \end{bmatrix} \tag{1}$$

$$\begin{bmatrix} \overline{\overline{S}}_H \\ \overline{B} \end{bmatrix} = \begin{bmatrix} s_H & d_H \\ d_H & \mu_T \end{bmatrix} \begin{bmatrix} \overline{\overline{T}}_H \\ \overline{H} \end{bmatrix}. \tag{2}$$

Equation (1) is the piezoelectric strain equation, and (2) is the magnetostrictive strain equation. The notation of parameters in (1) and (2) is listed as follows:

$\overline{\overline{T}}_{E,H}$: stress field tensors in the piezoelectric layer and magnetostrictive layer, respectively, with units of Newton/m^2. The subscript E indicates the corresponding parameters measured under constant-electric-field condition, and similarly, subscript H indicates constant-magnetic-field condition.

$\overline{\overline{S}}_{E,H}$: strain field tensors in the piezoelectric layer and magnetostrictive layer, respectively, with unit 1.

$\overline{E}$, $\overline{H}$: electric and magnetic field intensity vectors.

$\overline{D}$, $\overline{B}$: electric and magnetic flux density vectors.

ε_T, μ_T: stress-free permittivity of the piezoelectric layer, and stress-free permeability of the magnetostrictive layer, respectively.

s_E, s_H: mechanical compliance constants of the piezoelectric layer and magnetostrictive layer, respectively, with units of m^2/Newton. Both these two parameters are fourth-rank tensors representing the mechanical elasticity (inverse of the stiffness) of the material. In nonpiezoelectric and nonmagnetostrictive materials, compliance is the ratio between the strain and the stress, e.g., $S_{ij} = s_{ijkl}T_{kl}$ [23].

d_E, d_H: strain constants of the piezoelectric layer with units of coulombs/Newton, and magnetostrictive layer, with units of meter/Ampere, respectively. These two parameters are also called the piezoelectric and piezomagnetic coefficients, and both are third-rank tensors. In zero-electric-field and zero-magnetic-field case, $D_i = d_{Eijk}T_{jk}$ and $B_i = d_{Hijk}T_{jk}$.

For simplicity, it is assumed that all the field variables are unidirectional in the horizontal plane and the strain and stress are uniform within each layer. The boundary conditions at the interface in the stationary state are $\overline{\overline{S}}_E = \overline{\overline{S}}_H$ and $\overline{\overline{T}}_E = -\overline{\overline{T}}_H$. One can then merge (1) and (2) by eliminating the mechanical field variables, which yields

$$\begin{bmatrix} \overline{D} \\ \overline{B} \end{bmatrix} = \begin{bmatrix} \varepsilon_T - \frac{d_E^2}{s_E+s_H} & \frac{d_E \cdot d_H}{s_E+s_H} \\ \frac{d_E \cdot d_H}{s_E+s_H} & \mu_T - \frac{d_H^2}{s_E+s_H} \end{bmatrix} \begin{bmatrix} \overline{E} \\ \overline{H} \end{bmatrix}. \tag{3}$$

Equation (3) is in the form of the constitutive relations of the well-known bianisotropic magnetoelectric material [28], where the electromagnetic flux densities and fields are cross-coupled. In a dynamic strain-mediated system, however, the bianisotropic relations described by (3) do not hold in general, because strain and stress are often functions of time and space. Consequently, discussion of the dynamic properties of multiferroic materials must consider dynamic, bilateral interactions between electrodynamics and mechanical dynamics. For this purpose, the 1-D form of (1) and (2) is rewritten as

$$T = -\frac{e_D}{\varepsilon_S}D + c_D S, \quad E = \frac{1}{\varepsilon_S}D - \frac{e_D}{\varepsilon_S}S \tag{4}$$

$$T = -\frac{e_B}{\mu_S}B + c_B S, \quad H = \frac{1}{\mu_S}B - \frac{e_B}{\mu_S}S \tag{5}$$

with the following parameter notation:

e_D, e_B: stress constants of the piezoelectric layer, with units of coulombs/m^2, and magnetostrictive layer, with units of Newton/(Ampere·meter), respectively. The subscript D indicates the corresponding parameters measured under constant-electric-flux-density condition, and similarly, subscript B indicates constant-magnetic-flux-density condition. These two parameters are related to those in (1) and (2) by $e_D = d_E/s_E = d_E \cdot c_E$ and $e_B = d_H/s_H = d_H \cdot c_H$.

c_E, c_H: Young's moduli (or mechanical stiffness constants) of the piezoelectric layer and magnetostrictive layer, respectively, with units of Newton/m^2. These two parameters are related to those in (1) and (2) by $c_E = 1/s_E$ and $c_H = 1/s_H$.

c_D, c_B: mechanical stiffness constants of the piezoelectric layer and magnetostrictive layer, respectively, with units of Newton/m^2.

ε_S, μ_S: strain-free permittivity of the piezoelectric layer, and strain-free permeability of the magnetostrictive layer, respectively. These parameters are related to the constant-electromagnetic-field and constant-stress parameters through the following:

$$\begin{cases} c_D = \dfrac{c_E}{1-k_E^2} \\ c_B = \dfrac{c_H}{1-k_H^2} \end{cases}, \quad \begin{cases} \varepsilon_S = \varepsilon_T\left(1-k_E^2\right) \\ \mu_S = \mu_T\left(1-k_H^2\right) \end{cases} \tag{6}$$

where k_E^2 and k_H^2 are, respectively, electromechanical and magnetomechanical coupling figures of merits, given by

$$k_E^2 = \frac{d_E^2}{s_E \varepsilon_T}, \quad k_H^2 = \frac{d_H^2}{s_H \mu_T}. \tag{7}$$

The definition of energy in a multiferroic system may vary depending on which field quantities are viewed as the independent variables in the equation. As a consequence, an energy formulation can be obtained in terms of either stress or strain for the mechanical variables or in terms of flux density or field density for the electromagnetic terms. In this discussion, we write the mechanical energy in terms of stress and the electromagnetic energy in terms of the flux density. Using the magnetostrictive layer as an example, an alternative form of (2) can be written as

$$S = s_B T + \frac{d_H}{\mu_T} B, \quad H = -\frac{d_H}{\mu_T} T + \frac{1}{\mu_T} B. \tag{8}$$

The total stored energy W_{Total} in the magnetic phase of the system according to this definition is given by

$$\begin{aligned} W_{Total} &= \frac{1}{2}\iiint S \cdot T dv + \frac{1}{2}\iiint B \cdot H dv \\ &= \frac{1}{2}\iiint s_B |T|^2 dv + \frac{1}{2}\iiint \frac{|B|^2}{\mu_T} dv \end{aligned} \tag{9}$$

where $s_B = 1/c_B = (1-k_H^2)s_H$ is the mechanical compliance defined for constant magnetic flux density. Note that the total energy input to the system is now stored as a summation of the mechanical energy in the form of mechanical stress $W_T = \frac{1}{2}\iiint s_B |T|^2 dv$, and the magnetic energy in the form of magnetic flux density $W_B = \frac{1}{2}\iiint \frac{|B|^2}{\mu_T} dv$. The weak magnetic field condition holds when $|H| \ll \frac{|B|}{\mu_T}$, as will be seen in the following proposed antenna system. In this case, the energy in the system established by or released to the external magnetic field can be a small fraction of what is in the system stored in the form of magnetic flux density, e.g.,

$$\left|\frac{1}{2}\iiint B \cdot H dv\right| \ll W_B = \frac{1}{2}\iiint \frac{|B|^2}{\mu_T} dv. \tag{10}$$

This relation leads to the observation that the input of the energy to the system is primarily mechanical, while the stored energy is in the forms of both mechanical stress and magnetic flux density, due to the fact that part of the mechanical energy is transferred to magnetic energy. This is illustrated by

$$\begin{aligned} W_{Total} \approx \frac{1}{2}\iiint S \cdot T dv &= \frac{1}{2}\iiint s_B |T|^2 dv \\ &\quad + \frac{1}{2}\iiint \frac{|B|^2}{\mu_T} dv. \end{aligned} \tag{11}$$

On the other hand, it is obvious under the weak magnetic field assumption that $H \approx 0$ and $B \approx d_H T$, as derived from the second equation in (8). Substituting this relationship into (9) results in

$$\begin{aligned} W_{Total} &= \frac{1}{2}\iiint s_B |T|^2 dv + \frac{1}{2}\iiint \frac{d_H^2}{\mu_T} |T|^2 dv \\ &= \frac{1}{2}\iiint s_H |T|^2 dv. \end{aligned} \tag{12}$$

Multiplying (12) with $\left(1-k_H^2\right)$, then subtracting it from (9) yields

$$W_{Total} = \frac{1}{k_H^2}\frac{1}{2}\iiint \frac{|B|^2}{\mu_T} dv = \frac{1}{k_H^2} W_B. \tag{13}$$

The magnetomechanical coupling figure of merit k_H^2, defined by (7), thus has a very clear physical meaning as the maximum ratio of the mechanical energy input that can be transferred to magnetic energy and stored in the form of magnetic flux density. It thus carries a fundamental limit of $k_H^2 \leq 1$ to satisfy the energy conservation. Similar discussions can be carried out to describe the stored energy in a piezoelectric system and the mechanical-to-electric energy transfer relation.

III. Strain-Mediated Radiation

The essence of the proposed strain-mediated antenna is to create dynamic magnetic flux that is parallel to a conducting plane to electromagnetically radiate away from the conducting plane. The dynamic magnetic flux replaces the typical conductive current as the source of radiation in this case. The platform effect in the conventional current-based antennas is associated with the excessive energy storage in the platform and results in elevated radiation Q factors. Consequently, the performance bound of the proposed antenna must also be examined with regard to its radiation Q factor.

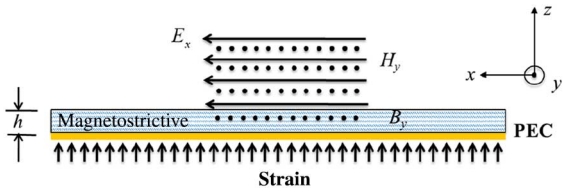

Fig. 2. Strain-mediated radiation in the magnetostrictive layer. The coordinate system is chosen such that the magnetic flux is in the y-direction. The thickness of the substrate satisfies the condition $\mu_r k_0 h \ll 1$.

To derive such a performance bound, it is assumed that a thin layer of magnetostrictive material on a perfect electrically conducting (PEC) ground plane is excited by a vertical dynamic strain. The structure is assumed to be homogeneous and extending to infinity in the horizontal directions, as depicted in Fig. 2. In Fig. 2, it is assumed that the dynamic strain is coupled through the ground plane and transferred uniformly onto the magnetostrictive layer. The dynamic strain excites a uniform dynamic magnetic flux within the magnetic layer. According to Faraday's law, this dynamic magnetic flux generates a dynamic electric field which varies linearly along the thickness dimension until it reaches above the surface of the magnetostrictive layer where an aperture electric field is formed. Denoting the aperture electric field by E_0, the average radiated power of the electromagnetic wave is thus calculated to be

$$P_{rad} = \frac{1}{2\eta_0} \iint_s |E_0|^2 ds. \tag{14}$$

Using Faraday's law $|B| = \frac{|E_0|}{(\omega h)} = \frac{|E_0|}{ck_0 h}$, where c is the speed of light and k_0 is the free-space wavenumber, the stored energy in the form of magnetic flux density in the magnetostrictive layer is derived to be

$$W_B = \frac{1}{2} \iiint_{0<z<h} \frac{|B|^2}{\mu_T} dv \approx \frac{h}{2(\omega h)^2 \mu_T} \iint_s |E_0|^2 ds. \tag{15}$$

The total stored energy includes an additional component in the form of mechanical stress as evidenced by (9). Joining the free-space radiation boundary condition $H = \frac{E_0}{\eta_0} = \frac{E_0}{c\mu_0}$ and Faraday's law, it is not difficult to show that the weak magnetic field condition $|H| \ll \frac{|B|}{\mu_T}$ holds when $\mu_r k_0 h \ll 1$. The total stored energy can thus be well represented by (13). The radiation quality factor is thus derived by substitution of (13) into

$$Q_{bound} = \omega \frac{W_{Total}}{P_{rad}} = \omega \frac{W_B / k_H^2}{P_{rad}} = \frac{1}{k_H^2} \frac{1}{\mu_r k_0 h} = \frac{s_H}{d_H^2} \frac{\mu_0}{k_0 h}. \tag{16}$$

Equation (16) actually represents the lower bound of the radiation Q factor for the proposed strain-mediated antenna when the stored energy in the magnetostrictive layer is the primary form of the stored energy. The stored energy considered for the above derivation does not include the near field above the antenna structure, nor the energy stored in the feeding structure beneath the ground plane. A complete antenna may involve stored energy in other parts and consequently a higher radiation quality factor may emerge. On the other hand, it is evident in (16) that the lower bound of the radiation Q factor decreases with higher permeability and higher mechanical-to-magnetic coupling factor k_H^2 of the magnetostrictive material. The concept of utilizing high-permeability magnetic material to lower the radiation quality factor is consistent with approaches attempted in [3]–[5]. The strain-mediated multiferroic approach offers further benefits associated with the absence of Ohmic losses due to the current conduction and the ease of impedance matching in the vertical direction through acoustic wave resonances.

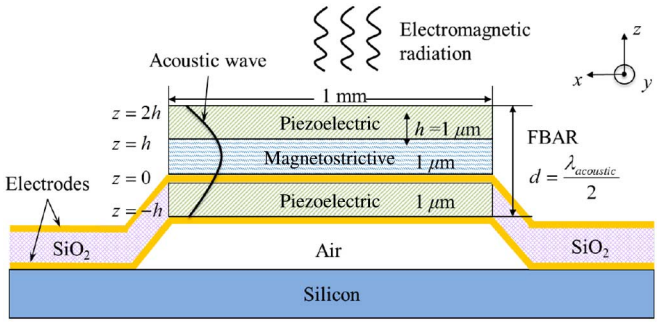

Fig. 3. BAW-resonance-based antenna. Electric current excitation is applied to the electrodes on both sides of the bottom piezoelectric layer, and it triggers the BAW resonance through converse piezoelectric effect.

IV. BAW-Mediated Multiferroic Antennas

The structure of the BAW resonator is exploited here to create dynamic strain and to couple it to the radiating element. BAW resonators based on either Bragg reflectors or film bulk acoustic resonance (FBAR) architectures have been extensively used by the RF filter community to create high-performance, low-loss RF filters with small form factors [24]. Here, the vertical stress and strain profile of BAW at resonance is leveraged to couple the dynamic strain from the piezoelectric phase to the magnetostrictive phase, while the horizontal dimensions allow scaling of the radiating elements, which is retained to satisfy certain impedance and gain requirements in practical antenna applications.

Shown in Fig. 3 is the proposed structure of a multiferroic antenna operating in the GHz regime, which consists of a three-layer strain-mediated BAW structure. An air cavity such as those in FBAR is placed underneath the layered structure to overcome the mechanical clamping effect of the substrate. The three layers include a magnetostrictive layer sandwiched between two piezoelectric layers. The bottom piezoelectric layer serves as the excitation layer. Current injection in the bottom piezoelectric excites an acoustic wave in the layered structure. The operating frequency of the antenna is chosen to be the BAW resonance frequency. The BAW resonance is established by the total thickness when it is approximately a multiple of a half-wavelength of the vertically propagating acoustic wave. For example, a 3-μm-thick layered structure has a lowest BAW resonance mode at approximately 1 GHz using the material parameters introduced in Section V-B.

The fundamental resonant mode maximizes the stress in the magnetostrictive layer as indicated in the half-period sinusoidal stress profile shown in Fig. 3. This allows the maximum strain to be imposed on the magnetostrictive layer for the purpose of generating a strong dynamic magnetic flux. To analyze the radiation quality factor of this structure, the energy stored in the complete sandwiched structure must be considered including energy stored in both the magnetostrictive and piezoelectric phases. Due to the open-circuit excitation of the piezoelectric layer ($D = 0$) after the initial current pulse drive and the weak magnetic field condition in the magnetostrictive layer ($|H| \ll \frac{|B|}{\mu_T}$ implies $H \approx 0$), the exchange of electric energy and magnetic energy with the outside world is negligible compared to the stored energy. The stored energy can thus be represented by the total stored mechanical energy. This is only expressed as a function of the stress induced under the conditions of constant electric flux density in the piezoelectric material and constant magnetic field in the magnetostrictive material as shown in (12)

$$W_{Total} = \frac{1}{2} \iiint\limits_{-h<z<0 \& h<z<2\,h} s_D |T|^2 dv + \frac{1}{2} \iiint\limits_{0<z<h} s_H |T|^2 dv = 2W_{PE} + W_{PM} \tag{17}$$

where W_{PE} and W_{PM} are the stored mechanical energies in each of the piezoelectric and magnetic layers. If the mechanical compliance of the piezoelectric layer is approximately the same as that in the magnetostrictive layer, the stored energy in these two phases are proportional according to the square of the vertical stress profile in the structure at the resonance, as shown by (18). Given the stress field distribution of $T = T_0 \sin(2\pi z/\lambda_{ac})$ and the resonance condition $\lambda_{ac} = 2d = 6\,h$ where λ_{ac} is the wavelength of the acoustic wave, the total stored mechanical energy in the three layers is thus

$$\begin{aligned} W_{Total} &= \frac{1}{2} \iiint\limits_{-h<z<2\,h} s_H |T|^2 dv \\ &= \frac{1}{2} s_H T_0^2 \cdot A \cdot \int_0^d \sin^2\left(\frac{2\pi}{\lambda_{ac}} z\right) dz \\ &= \frac{1}{2} s_H T_0^2 \cdot A \cdot \frac{\lambda_{ac}}{2\pi} \int_0^\pi \sin^2(x)\, dx \\ &= \frac{3}{2} W_{TU} \end{aligned} \tag{18}$$

where A is the surface area of the BAW structure and W_{TU} is the stored energy calculated from (12) by applying a uniform stress distribution, e.g.,

$$W_{TU} = \frac{1}{2} s_H T_0^2 \cdot A \cdot h. \tag{19}$$

In addition to the elastic energy stored in the form of mechanical stress, the energy in an acoustic resonator should include an equal amount of kinetic energy. The radiation quality factor of the BAW structure is thus derived as

$$\begin{aligned} Q_a &= \omega \frac{2W_T}{P_{rad}} = \omega \frac{3W_{TU}}{P_{rad}} \\ &= 3Q_{bound} \end{aligned} \tag{20}$$

and Q_{bound} is the lower bound of the radiation Q given by (16).

V. 1-D FDTD Modeling

In a dynamic multiferroic system, the behaviors of acoustic waves and electromagnetic waves are, respectively, governed by Newton's laws and Maxwell's equations as follows:

$$\nabla \cdot \overline{\overline{T}} = \rho \frac{\partial \overline{v}}{\partial t}, \quad \nabla_S \overline{v} = \frac{\partial \overline{\overline{S}}}{\partial t} \tag{21}$$

$$\nabla \times \overline{E} = -\frac{\partial \overline{B}}{\partial t}, \quad \nabla \times \overline{H} = \sigma \overline{E} + \frac{\partial \overline{D}}{\partial t}. \tag{22}$$

In (21), $\overline{v}$ is the particle velocity vector, which is the instantaneous velocity of the group of atoms or molecules in material that vibrate in a uniform way. ρ is the mass density of the material and σ is the conductivity. The behavior of the BAW-mediated multiferroic antenna can thus be predicted with an FDTD algorithm that jointly solves these two sets of equations. Due to the thin profile of the structure, both the magnetostrictive and piezoelectric layers are assumed to extend to infinity in the film plane with uniform strain and stress field distributions. The FDTD modeling proposed here is thus 1-D. The purpose of this model is not to design a practical antenna structure but to understand the fundamental physics and coupling between the electromagnetics and dynamic mechanics. Therefore, Newton's law (21) and Maxwell's equations (22) are reduced to their 1-D forms, respectively,

$$\begin{aligned} \frac{\partial T}{\partial z} &= \rho \frac{\partial v}{\partial t}, \quad \frac{\partial v}{\partial z} = \frac{\partial S}{\partial t} \\ \frac{\partial E}{\partial z} &= \frac{\partial B}{\partial t}, \quad \frac{\partial H}{\partial z} = \sigma E + \frac{\partial D}{\partial t}. \end{aligned} \tag{23}$$

A. 1-D Multiscale FDTD Algorithm

The bilateral interactions between the acoustic waves and electromagnetic waves are thus modeled by substituting the strain-mediated constitutive relations (4) and (5) into (23). The combination of (4) and (23) leads to 1-D differential equations in the piezoelectric layer

$$\frac{\partial E}{\partial t} = -\frac{e_D}{\varepsilon_S} \frac{\partial v}{\partial z} + \frac{1}{\varepsilon_S} \frac{\partial D}{\partial t} \tag{24}$$

$$\frac{\partial T}{\partial t} = c_D \frac{\partial v}{\partial z} - \frac{e_D}{\varepsilon_S} \frac{\partial D}{\partial t} \tag{25}$$

where the electric flux density D serves as the excitation. Similarly, the combination of (5) and (23) leads to 1-D differential equations in the magnetostrictive layer

$$\frac{\partial H}{\partial t} = -\frac{e_B}{\mu_S} \frac{\partial v}{\partial z} + \frac{1}{\mu_S} \frac{\partial B}{\partial t} \tag{26}$$

$$\frac{\partial T}{\partial t} = c_B \frac{\partial v}{\partial z} - \frac{e_B}{\mu_S} \frac{\partial B}{\partial t}. \tag{27}$$

In order to solve the equations in (23) simultaneously, the FDTD method must perform time marching for both the electromagnetic field variables and the mechanical field variables at the same time steps. However, as the wavelength of an acoustic wave is approximately five orders of magnitude smaller than that of an electromagnetic wave at the same frequency, the drastic difference between the spatial scales of these two types of

waves gives rise to a numerical issue. In order to retain the spatial resolution for acoustic waves, the spatial grids need to be divided based on the smaller wavelength of the two waves, which is the acoustic wavelength. Therefore, the spatial grid is typically no more than one-tenth of the acoustic wavelength. In order to satisfy the stability condition, the time steps must be defined according to the shorter traveling time of the two waves when they cross each spatial grid, which is

$$\Delta t = \min\left(\frac{\Delta z_{ac}}{c}, \frac{\Delta z_{ac}}{v_{ac}}\right). \tag{28}$$

Note that $c/v_{ac} \approx 10^5$; it is thus concluded that Δt must be much smaller than the RF cycle, which would lead to severe oversampling in time-domain and extremely poor computational efficiency. To avoid this oversampling issue, different spatial scales are applied to these two different waves. For electromagnetic waves, due to its large wavelength, one may use a much sparser grid than that of the acoustic waves to describe its spatial behavior and then interpolate the electromagnetic field inside the large grid with polynomial basis functions to match the field variables of the acoustic waves. This leads to the reduction in the number of unknowns for electromagnetic field variables and avoids the stability problem or oversampling problem. Specific to the 1-D FDTD algorithm implemented for thin-film structures, a single grid is needed to represent the electromagnetic field in the magnetic material and the following polynomial spatial expansion is used to derive the field on the acoustic wave grid:

$$B_x = B_{x0}, \quad H_x = H_{x0}, \quad E_y = E_{y1} z \tag{29}$$

where B_{x0}, H_{x0}, and E_{y1} are unknowns to be solved by 1-D FDTD. If more dramatic electromagnetic field variation is expected, higher order terms could be added to (29) for better accuracy. With (29), Faraday's law in (23) reduces to

$$\frac{\partial B_x}{\partial t} = \frac{\partial E_y}{\partial z} = E_{y1}. \tag{30}$$

The radiation boundary condition takes the form

$$\left.\frac{E_y}{H_x}\right|_{z=h} = -\eta_0 \tag{31}$$

which yields

$$\frac{\partial H_x}{\partial t} = -\frac{1}{\eta_0}\left.\frac{\partial E_y}{\partial t}\right|_{z=h} = -\frac{h}{\eta_0}\frac{\partial E_{y1}}{\partial t}. \tag{32}$$

Substituting (30) to (26) gives

$$E_{y1} = \mu_S \frac{\partial H_x}{\partial t} + e_B \frac{\partial v}{\partial z}. \tag{33}$$

With (32) substituted into (33) to eliminate $\frac{\partial H_x}{\partial t}$ and (30) substituted into (27) to eliminate $\frac{\partial B_x}{\partial t}$, one obtains the following two differential equations:

$$\frac{\mu_S h}{\eta_0}\frac{\partial E_{y1}}{\partial t} + E_{y1} = e_B \frac{\partial v}{\partial z} \tag{34}$$

$$\frac{\partial T}{\partial t} = c_B \frac{\partial v}{\partial z} - \frac{e_B}{\mu_S} E_{y1}. \tag{35}$$

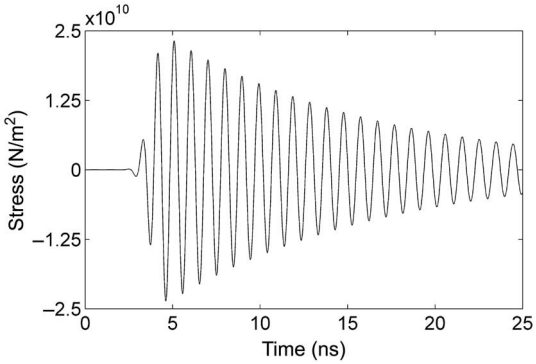

Fig. 4. Dynamic stress field in the middle line of the proposed BAW-mediated multiferroic antenna structure shown in Fig. 3.

These two equations are solved jointly with the following Newton's equation:

$$\frac{\partial T}{\partial z} = \rho \frac{\partial v}{\partial t}. \tag{36}$$

Note that (36) applies to the whole structure, including both the piezoelectric and the magnetostrictive layers. Equations (34) and (35) are replaced by the following equations in the piezoelectric layer:

$$\frac{\partial D}{\partial t} = \varepsilon_S \frac{\partial E_z}{\partial t} + e_D \frac{\partial v}{\partial z} \tag{37}$$

$$\frac{\partial T}{\partial t} = c_D \frac{\partial v}{\partial z} - \frac{e_D}{\varepsilon_S}\frac{\partial D}{\partial t}. \tag{38}$$

The leap-frog time-stepping scheme in FDTD can now be implemented to discretize equations (34)–(38) in spatial and temporal domain, which leads to

$$E_{y1}^{n+1/2} = \frac{\frac{\mu_S h}{\eta_0 \Delta t} - 0.5}{\frac{\mu_S h}{\eta_0 \Delta t} + 0.5} E_{y1}^{n-1/2} + mean\left\{\frac{e_B}{0.5 + \frac{\mu_S h}{\eta_0 \Delta t}} \frac{v_{i+1/2}^n - v_{i-1/2}^n}{\Delta z}\right\} \tag{39}$$

$$T_i^{n+1/2} = T_i^{n-1/2} + c_B \frac{v_{i+1/2}^n - v_{i-1/2}^n}{\Delta z}\Delta t - \frac{e_B}{\mu_S}\frac{E_{y1}^{n+1/2} + E_{y1}^{n-1/2}}{2}\Delta t \tag{40}$$

for the magnetostrictive layer, and

$$T_i^{n+1/2} = T_{i-1}^{n-1/2} + \frac{c_D \Delta t}{\Delta z}\left(v_{i+1/2}^n - v_{i-1/2}^n\right) - \frac{e_D}{\varepsilon_S}\left(D_i^{n+1/2} - D_i^{n-1/2}\right) \tag{41}$$

$$E_{zi}^{n+1/2} = E_{zi}^{n-1/2} - \frac{e_D \Delta t}{\varepsilon_S \Delta z}\left(v_{i+1/2}^n - v_{i-1/2}^n\right) + \frac{1}{\varepsilon_S}\left(D_i^{n+1/2} - D_i^{n-1/2}\right) \tag{42}$$

for the piezoelectric layers, and

$$v_{i+1/2}^{n+1} = v_{i+1/2}^n + \frac{\Delta t}{\rho \Delta z}\left(T_i^{n+1/2} - T_{i-1}^{n+1/2}\right) \tag{43}$$

for both phases.

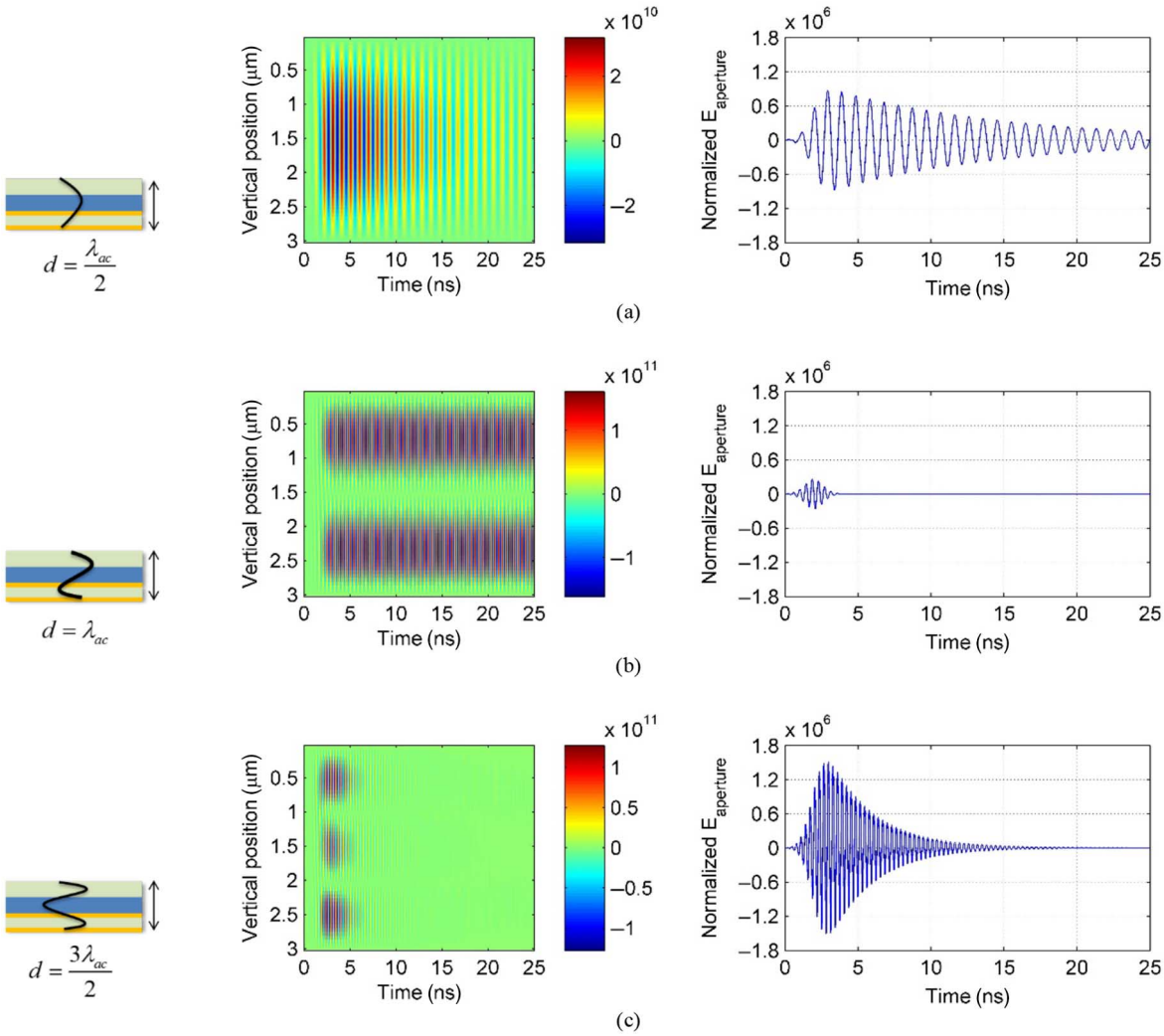

Fig. 5. First column: standing wave distribution of the stress field in the vertical direction for the first three BAW resonant modes. Second column: stress profiles throughout the BAW structure as a function of time. Third column: normalized aperture electric field. (a) $f = 1.03$ GHz. (b) $f = 2.28$ GHz. (c) $f = 3.17$ GHz.

In the magnetostrictive layer, (39) describes the time marching of the aperture electric field as a function of the particle velocity. Both the electric field and the particle velocity are used to update the stress in (40) and then the particle velocity is updated from stress in (43). An electrical flux density in the form of a modulated Gaussian pulse $D(t) = \exp\left[-(t-t_0)^2/2T^2\right]\cos(2\pi f t)$ is applied through the vertical direction of the bottom piezoelectric layer to excite the resonance. In the piezoelectric layer, the vertical electric flux density is used with the particle velocity to update the stress in (41), the vertical electric field is then updated with the electric flux density excitation and the particle velocity in (42), and ultimately the particle velocity is updated with the stress in (43).

B. Simulation Results

For simplification of discussions, the BAW structure to be simulated is assumed to contain only nondispersive and lossless material. The mechanical property of the material is matched to those of typical ferrite and piezoelectric material. For example, the magnetostrictive material is assumed to have a similar mechanical property to that of yttrium iron garnet (YIG) and the piezoelectric material is assumed with a similar mechanical property to that of zinc oxide (ZnO). The following are the material properties assumed for the simulation: $\varepsilon_T = 12.64\varepsilon_0$, $\mu_T = 2000\mu_0$, $c_D = 2.3032 \times 10^{11}$ (N/m^2), $c_H = 2.11 \times 10^{11}$ (N/m^2), $d_H = 1.04 \times 10^{-7}$ (m/A), $d_D = 11.67 \times 10^{-12}$ (C/N), $e_D = 1.32$ (C/m^2), $\rho_E = 5.68 \times 10^3$ (kg/m^3), and $\rho_H = 5.17 \times 10^3$ (kg/m^3). It should be noted that the dynamic permeability and the piezomagnetic coefficients of the magnetostrictive material are artificially adjusted to study the effects of those parameters critical to the antenna performance. The aforementioned material properties lead to a magnetomechanical coupling figure of merit $k_H^2 = 0.9080$. The central frequency of the excitation is $f = 1.0$ GHz with a bandwidth of ± 300 MHz. With the electromagnetic unknown reduction strategy, the time step and spatial grid can now be defined based on the properties of BAW

$$\Delta z = \frac{\lambda_{ac}}{108} \approx 50 \text{ nm}, \quad \Delta t = \frac{\Delta z}{v_{ac}} \frac{1}{16} \approx 50 \text{ ps}. \tag{44}$$

The electromagnetic radiations, i.e., the mechanical energy released to free space, can be observed from the simulation results in Figs. 4 and 5. Fig. 4 shows the dynamic stress waveform at the center of the magnetostrictive layer of the structure shown in Fig. 3, excited by the modulated Gaussian pulse input. The amplitude of the standing stress field decays due to the electromagnetic radiation. It implies that the radiation of electromagnetic waves acts as a damping load to the acoustic wave resonances. The middle column of Fig. 5 plots the vertical stress profile in the three-layer BAW structure as a function of time, for the first three resonant modes. It is observed that the damping of the resonance as the consequence of electromagnetic radiation occurs when the mechanical strain is maximized in the middle layer, as shown in Fig. 5(a) and (c). However, when there is a null of the strain profile in the middle layer, very little damping is observed, which is shown in Fig. 5(b). The third column of Fig. 5 shows the aperture electric field above the antenna structure as a function of time normalized by the input energy. It can be observed that the normalized radiated field intensity for the second BAW resonant mode is indeed negligible compared with that of the other two modes. This further validates the concept that the electromagnetic radiation is created only through the dynamic magnetic flux generated by the strain excitation.

Radiation quality factors are derived from the simulated stress waveform by extracting the damping speed of the resonance incurred by the electromagnetic radiation with the signal processing code ESPRIT [29]. Based on the aforementioned material property setting, the theoretical lower bound of radiation Q factor is 25.5 according to (16), which corresponds to the analytical radiation Q of 76.4 for the BAW-mediated antenna. The simulated radiation Q factor of the antenna with FDTD code is 77.9, which is very close to the analytical result. In general, the simulated radiation Q factor matches well with the analytical radiation Q factor for different permeability settings and magnetomechanical coupling figures of merit as shown in Fig. 6. The agreement between the numerical solutions and the analytic solutions validates both the operating principle of the proposed antenna structure and the FDTD algorithm developed for solving such a multiphysics problem. Furthermore, it shows that a relative permeability of 2000 and a magnetomechanical coupling greater than 85% in the magnetostrictive material could lead to efficient radiation (with radiation Q factor of below 100) at 1.03 GHz even with a 1-μm-thick layer of magnetostrictive material.

The antenna input impedance and radiation resistance as functions of frequency are calculated with different methods with both results plotted in Fig. 7 for comparison. The antenna input impedance is calculated by taking the ratio of the input voltage to the excitation displacement current. The input voltage is obtained by performing the line integral of vertical electric field through the bottom piezoelectric layer, and the excitation displacement current is computed by $I = A\,(\partial D/\partial t)$. The radiation resistance is calculated using the ratio between the radiated power obtained with (14) and the square of the excitation displacement current. In Fig. 7, the input resistance agrees well with the radiation resistance, even

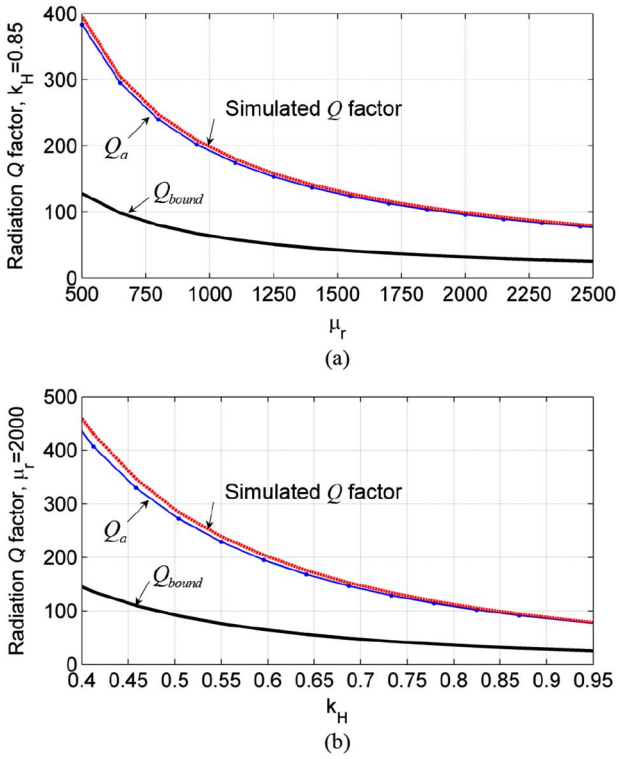

Fig. 6. (a) Simulated radiation Q factor compared to the theory for different permeability, $k_H = 0.85$. (b) Simulated radiation Q factor compared to the theory for different magnetomechanical coupling figure of merits, $\mu_r = 2000$. Parameters in Fig. 4 apply.

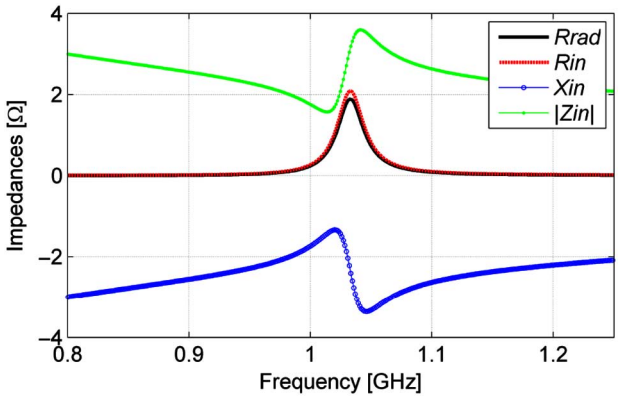

Fig. 7. Input impedance and radiation resistance for a reference area of 1 mm^2.

though they are obtained with different approaches. This agreement has further validated the FDTD simulation method. The simulated radiation resistance is 1.9 Ω per square millimeter near BAW resonance.

The radiated power from such an antenna might be limited by the saturation effect of the magnetic material. To operate the antenna in the linear regime, the dynamic magnetic field within the ferrite must be perpendicular to the direction of the applied dc magnetic field bias that is used to saturate the material. It should also be smaller than the saturation field in its magnitude, i.e., $H_{dynamic} \ll H_{dc}$, so that the small signal approximation

to the Landau–Lifshitz–Gilbert (LLG) equation [31] can hold. For example, in YIG, the common value of the dc field to saturate the material is 50 Oe, which will give an upper limit of 0.5 Oe to the dynamic magnetic field. The radiated power per square millimeter in this condition is obtained to be

$$P_{rad} = \frac{\eta_0 H_{dynamic}^2}{2} \cdot 10^{-6} = 0.3 \text{ W/mm}^2. \qquad (45)$$

Therefore, the proposed antenna may be able to radiate watts of power if it can be laid out over the area of a few square millimeters or less if material with higher saturation magnetic field is used.

VI. Conclusion

Multiferroic antennas based on the dynamic interactions of electromagnetic and acoustic waves open up a new territory in conformal antenna design. BAW resonator structures are proposed to form effective dynamic strain coupling to a thin magnetostrictive layer, which may generate the dynamic magnetic flux needed for electromagnetic wave radiation. A 1-D multiscale FDTD code is developed to model the proposed antenna structure. Numerical results agree well with the analytical results, which validates both theoretical and numerical analyses. The analyses conclude that with an increase in the dynamic permeability in the magnetic layer and a reasonable magnetomechanical coupling figure of merit, the proposed BAW-based multiferroic antenna can achieve a low radiation Q that can lead to high efficiency radiation required for practical antenna deployment.

References

[1] J. C.-E. Sten, A. Hujanen, and P. K. Koivisto, "Quality factor of an electrically small antenna radiating close to a conducting plane," *IEEE Trans. Antennas Propag.*, vol. 49, no. 5, pp. 829–837, May 2001.

[2] D. M. Pozar, "Microstrip Antennas," *Proc. IEEE*, vol. 80, no. 1, pp. 79–81, Jan. 1992.

[3] R. C. Hansen and M. Burke, "Antennas with magneto-dielectrics," *Microw. Opt. Technol. Lett.*, vol. 2, pp. 75–78, 2000.

[4] H. Mosallaei and K. Sarabandi, "Magneto-dielectrics in electromagnetics: Concept and applications," *IEEE Trans. Antennas Propag.*, vol. 52, no. 6, pp. 1558–1567, Jun. 2004.

[5] P. M. T. Ikonen, K. N. Rozanov, A. V. Osipov, P. Alitalo, and S. A. Tretyakov, "Magnetodielectric substrates in antenna miniaturization: Potential and limitations," *IEEE Trans. Antennas Propag.*, vol. 54, no. 11, pp. 3391–3399, Nov. 2006.

[6] N. Altunyurt, M. Swaminathan, P. M. Raj, and V. Nair, "Antenna miniaturization using magneto-dielectric substrates," in *Proc. 59th Electron. Compon. Technol. Conf.*, 2009, pp. 801–808.

[7] F. Namin, T. G. Spence, D. H. Werner, and E. Semouchkina, "Broadband, miniaturized stacked-patch antennas for L-band operation based on magneto-dielectric substrates," *IEEE Trans. Antennas Propag.*, vol. 58, no. 9, pp. 2817–2822, Sep. 2010.

[8] G.-M. Yang *et al.*, "Planar annular ring antennas with multilayer self-biased NiCo-ferrite films loading," *IEEE Trans. Antennas Propag.*, vol. 58, no. 3, pp. 648–655, Mar. 2010.

[9] X. M. Yang *et al.*, "Increasing the bandwidth of microstrip patch antenna by loading compact artificial magneto-dielectrics," *IEEE Trans. Antennas Propag.*, vol. 59, no. 2, pp. 373–378, Feb. 2011.

[10] N. A. Hill, "Why are there so few magnetic ferroelectrics?" *J. Phys. Chem. B*, vol. 104, no. 29, p. 6694, Jun. 2000.

[11] M. I. Bichurin *et al.*, "Theory of magnetoelectric effects at microwave frequencies in a piezoelectric magnetostrictive multilayer composite," *Phys. Rev. B*, vol. 64, no. 9, p. 094409, Aug. 2001.

[12] L. Mitoseriu and V. Buscaglia, "Intrinsic/extrinsic interplay contributions to the functional properties of ferroelectric-magnetic composites," *Phase Transitions*, vol. 79, no. 12, pp. 1095–1121, Dec. 2006.

[13] R. Ramesh and N. A. Spaldin, "Multiferroics: Progress and prospects in thin films," *Nat. Mater.*, vol. 6, no. 1, pp. 21–29, Jan. 2007.

[14] C. W. Nan, M. I. Bichurin, S. Dong, D. Viehland, and G. Srinivasan, "Multiferroic magnetoelectric composites: Historical perspective, status, and future directions," *J. Appl. Phys.*, vol. 103, no. 3, pp. 031101-1–031101-34, 2008, art. no. 031101.

[15] C. A. F. Vaz, J. Hoffman, C. H. Ahn, and R. Ramesh, "Magnetoelectric coupling effects in multiferroic complex oxide composite structures," *Adv. Mater.*, vol. 22, nos. 26–27, pp. 2900–2905, 2010.

[16] R. V. Petrov *et al.*, "Miniature antenna based on magnetoelectric composites," *Electron. Lett.* vol. 44, no. 8, pp. 506–508, Apr. 2008.

[17] G.-M. Yang *et al.*, "Electronically tunable miniaturized antennas on magnetoelectric substrates with enhanced performance," *IEEE Trans. Magn.*, vol. 44, no. 11, pp. 3091–3094, Nov. 2008.

[18] R. J. Miller, W. P. Geren, and S. P. Hubbell, "Multiferroic antenna/sensor," U.S. Patent 20 110 062 955, Mar. 17, 2011.

[19] R. D. Mindlin, "Electromagnetic radiation from a vibrating quartz plate," *Int. J. Solids Struct.*, vol. 9, no. 6, pp. 697–702, Jun. 1973.

[20] P. C. Y. Lee, "Electromagnetic radiation from an AT-cut quartz plate under lateral-field excitation," *J. Appl. Phys.*, vol. 65, no. 4, pp. 1395–1399, Feb. 1989.

[21] P. C. Y. Lee, "Electromagnetic radiation from doubly rotated piezoelectric crystal plates vibrating at thickness frequencies," *J. Appl. Phys.*, vol. 67, no. 11, pp. 6633–6642, Jun. 1990.

[22] R. B. Thompson, "A model for the electromagnetic generation of ultrasonic guided waves in ferromagnetic metal polycrystals," *IEEE Trans. Sonics Ultrason.*, vol. 25, no. 1, pp. 7–15, Jan. 1978.

[23] B. A. Auld, "Piezoelectricity," in *Acoustic Fields and Waves in Solids*, vol. 1, 2nd ed. Melbourne, FL, USA: Krieger, 1990, pp. 281–282.

[24] J. F. Rosenbaum, *Bulk Acoustic Wave Theory and Devices*. Norwood, MA, USA: Artech House, 1988.

[25] K. S. Yee, "Numerical solutions of initial boundary value problems involving Maxwell's equations in isotropic media," *IEEE Trans. Microw. Theory Techn.*, vol. AP-14, no. 8, pp. 302–307, May 1966.

[26] A. Taflove and S. C. Hagness, *Computational Electrodynamics: The Finite-Difference Time-Domain Method*, 2nd ed. Norwood, MA, USA: Artech House, 2000.

[27] K. Seo, S. Ju, and H. Kim, "The modeling of thin-film bulk acoustic wave resonators using the FDTD methods," *IEEE Electron Device Lett.*, vol. 23, no. 6, pp. 327–329, Jun. 2002.

[28] J. A. Kong, "Theorems of bianisotropic media," *Proc. IEEE*, vol. 60, no. 9, pp. 1036–1046, Sep. 1972.

[29] R. Roy and T. Kailath, "ESPRIT-estimation of signal parameters via rotational invariance techniques," *IEEE Trans. Acoust. Speech Signal Process.*, vol. 37, no. 7, pp. 984–995, Jul. 1989.

[30] Z. Yao and Y. Wang, "Dynamic analysis of acoustic wave mediated multiferroic radiation via FDTD methods," in *Proc. IEEE Int. Symp. Antennas Propag.*, Memphis, TN, USA, Jul. 6–11, 2014, pp. 731–732.

[31] D. M. Pozar, *Microwave Engineering*, 3rd ed. Hoboken, NJ, USA: Wiley, 2005.

Zhi Yao (S'14) was born in Laiwu, China, in 1991. She received the B.S. degree in optical engineering from Zhejiang University, Hangzhou, China, in 2012, and the M.S. degree in electrical engineering from the University of California, Los Angeles (UCLA), Los Angeles, CA, USA, in 2014. She is currently pursuing the Ph.D. degree in electrical engineering at UCLA.

From 2011 to 2012, she worked with the University of California, Davis (UCD), Davis, CA, USA, where she contributed to the development of an millimeter wave phased antenna array system. Since 2012, she has been working with the NSF funded Engineering Research Center, UCLA—Translational Applications of Nanoscale Multiferroic Systems (TANMS). Her research interests include numerical modeling of multiphysics interactions, novel material applications for antenna design, and multiferroics in RF applications.

Yuanxun Ethan Wang (S'96–M'99–SM'09) received the B.S. degree from the University of Science and Technology of China (USTC), Hefei, China, in 1993, and the M.S. and the Ph.D. degrees from the University of Texas at Austin, Austin, TX, USA, in 1996 and 1999, respectively, all in electrical engineering.

He became an Assistant Professor with the Department of Electrical Engineering, University of California, Los Angeles (UCLA) since 2002, and is now an Associate Professor with the same department. He has published more than 100 journal and conference papers. He is the Director of the Digital Microwave Laboratory and the Center for High Frequency Electronics (CHFE), Department of Electrical Engineering, UCLA, and the Leader of Antenna Thrust in National Science Foundation funded Engineering Research Center—Translational Applications of Nanoscale Multiferroic Systems (TANMS). His research interests include microwave systems with emphasis on the front-ends including antennas, phased arrays, high performance RF transmitters and receivers. His researches blend digital technologies and concepts into RF design, which often leads to novel antenna and circuit configurations with performances beyond the conventional bound.

Dr. Wang is an Associate Editor of IEEE TRANSACTIONS ON ANTENNAS AND PROPAGATION.

Scott Keller received the degrees in mathematics, physics, and engineering, and the Ph.D. degree in mechanical engineering from the University of California, Los Angeles (UCLA), Los Angeles, CA, USA, in 2013.

He is with the Institute for Technology Advancement, UCLA, and is involved with research for the NSF ERC, Translational Applications of Nanoscale Multiferroic Systems (TANMS). Prior to joining TANMS, he served as the Director of Research and Development for the medical device manufacturing company, Interface Associates and as the Engineering Manager and Senior Engineer for several academic research groups in the areas of advanced materials, fusion science and technology (at UCLA), and basic plasma physics research (at UCI). His publications and conference presentations include several articles on multiferroic materials. His research interests include wave propagation in multiferroic materials and modeling.

Dr. Keller is a member of ASME, SIAM, and SPIE.

Gregory P. Carman joined the Department of Mechanical and Aerospace Engineering, University of California, Los Angeles (UCLA), Los Angeles, CA, USA, in 1991. He is the Director of a new NSF Engineering Research Center entitled Translational Applications of Nanoscale Multiferroic Materials (TANMS) and is Executive Engineering Director of the Center for Advanced Surgical and Interventional Technology, Department of Surgery, UCLA. His research interests include analytical modeling, fabrication, and testing of multiferroic (magnetoelectric) materials and developing devices for medical applications.

Mr. Carman has served as Chairman for the Adaptive Structures and Material Systems of the ASME (2000–2002), holds a position as Associate Editor for the *Journal of Intelligent Material Systems and Structures* and *Smart Materials and Structures*. He was awarded the Northrop Grumman Young Faculty in 1995 and three Best Paper Awards from the ASME in 1996, 2001, and 2007. In 2003, he was elected to the grade of Fellow in ASME and awarded the ASME Adaptive Structures and Material Systems Prize honoring his contributions to smart materials and structures in 2004. In 2015, SPIE honored him with the SSM Lifetime Achievement Award.